HHS Public Access

Author manuscript

Urolithiasis. Author manuscript; available in PMC 2017 June 01.

Published in final edited form as:

Urolithiasis. 2016 June ; 44(3): 211–217. doi:10.1007/s00240-015-0834-9.

INTRALUMINAL MEASUREMENT OF PAPILLARY DUCT URINE pH, *IN VIVO:* A PILOT STUDY IN THE SWINE KIDNEY

Rajash K. Handa, **James E. Lingeman**, **Sharon B. Bledsoe**, **Andrew P. Evan**, **Bret A. Connors**, and **Cynthia D. Johnson**

Department of Anatomy and Cell Biology (RKH, SBB, APE, BAC, CDJ), Indiana University School of Medicine and Department of Urology (JEL), Indiana University Health at Methodist Hospital, Indianapolis, Indiana

Abstract

We describe the *in vivo* use of an optic-chemo microsensor to measure intraluminal papillary duct urine pH in a large mammal. Fiber-optic pH microsensors have a tip diameter of 140-μm that allows insertion into papillary Bellini ducts to measure tubule urine proton concentration. Anesthetized adult pigs underwent percutaneous nephrolithotomy to access the lower pole of the urinary collecting system. A flexible nephroscope was advanced towards an upper pole papilla with the fiber-optic microsensor contained within the working channel. The microsensor was then carefully inserted into Bellini ducts to measure tubule urine pH in real time. We successfully recorded tubule urine pH values in five papillary ducts from three pigs (1 farm pig and 2 metabolic syndrome Ossabaw pigs). Our results demonstrate that optical microsensor technology can be used to measure intraluminal urine pH in real time in a living large mammal. This opens the possibility for application of this optical pH sensing technology in nephrolithiasis.

Keywords

fiber-optic chemical sensor; hydrogen ion concentration; kidney; tubule; shock wave lithotripsy

INTRODUCTION

Increased urinary supersaturation of stone-forming salts is the driving force for the formation of crystalline particles and for many minerals is a pH-dependent process. Uric acid, cystine and calcium oxalate stones readily form in an acidic environment, whereas calcium phosphate (apatite or brushite), calcium carbonate and magnesium phosphate stones develop in an alkaline environment [1]. However, there are human nephrolithiasis conditions in which the mineral composition of tubular deposits and renal stones cannot be readily explained by supersaturation or pH values of bulk urine [2]. One suggestion is an alteration

Correspondence: Rajash K. Handa, Ph.D., rajash_handa@hotmail.com.

Compliance with Ethical Standards:

Conflict of Interest: Authors RKH, SBB, APE, BAC and CDJ declare no conflict of interest; JEL has investment interests with Midwest Mobile Lithotripsy and Midstate Mobile Lithotripsy.

Ethical approval: All applicable international, national, and/or institutional guidelines for the care and use of animals were followed.

in the tubule microenvironment (e.g. intraluminal urine pH), which influences the physiochemical properties of stone formation. Therefore, there is a need to be able to assess the microenvironment of collecting ducts in a living kidney using a technology that can be translated to stone formers.

Early work on luminal urine pH in collecting ducts was performed in anesthetized rodents and involved immobilizing the kidney in a Lucite cup and then surgically exposing the renal pelvis to access papillary collecting ducts for micropuncture or microcatheterization [3–5]. Such rodent studies have provided insights into distal tubule acidification processes within segments of the inner medullary collecting tubule to the papillary duct tip [4, 5]. However, these techniques for papillary collecting duct measurements are not feasible for large animals or patients.

Chemical sensor systems exist that allow the optical sensing of analytes including protons (i.e. pH) [6]. Such technology use very small fiber-optic microsensors (diameter size of 20–200 μm are typical), which could allow the potential pH measurement of renal tubule urine in real time, *in vivo*. The use of conventional endourological procedures to access the renal collecting system—that is, percutaneous nephrolithotomy or ureteroscopy—could be a means by which such sensors gain access to papillary collecting ducts. This would allow the potential *in vivo* use of optical sensors in large animal and human kidneys. Herein, we report our initial results using a fiber-optic pH microsensor in anesthetized pigs to determine whether such optical sensing technology can be used to measure intraluminal urine pH in renal papillary ducts.

METHODS

The study was done in accordance with the NIH Guide for the Care and Use of Laboratory Animals; and received Indiana University School of Medicine and Methodist Hospital Institutional animal care and use committee approval.

Fiber-optic pH microsensor

A fiber-optic phase detection system (PreSens, Regensburg, Germany) was used to measure fluid pH within the urinary system. The pH-1 micro system is composed of a light emitting diode with an excitation wavelength of 470-nm to excite the pH sensor; an optical fiber as signal transducer; a photomultiplier to detect emitted light from the sensor; and a chemo-optical sensor immobilized in a solid matrix at the fiber-optic tip (140-μm diameter; see Figure 1). The chemo-optic sensor consists of an H^+-insensitive, long decay time, reference luminophore and a H^+-sensitive, short decay time, indicator luminophore—the latter changes its fluorescence intensity due to dynamic quenching by H^+. The average decay time of the luminophores is measured, which represents the ratio of the two fluorescence intensities and allows conversion of fluorescence intensity into a phase shift. The average phase shift reflects the intensity of the indicator luminophore and, consequently, the H^+ concentration (i.e. pH value). Details on the principles of the system have been previously published [7, 8].

Renal tubule pH measurement, *in vivo*

Proof of concept—An initial pig experiment was performed to determine whether the fiber-optic pH microsensor system was sufficiently robust to be used in the measurement of renal tubular fluid, *in vivo*. A 70 kg female farm pig was anesthetized and prepared for percutaneous nephrolithotomy (PCNL) using routine clinical procedures [9]. Percutaneous access was achieved with an 18-gauge diamond-tipped access needle, which punctured a targeted lower pole calyx under biplanar fluoroscopic guidance. An 8/10 coaxial fascial dilator and NephroMax balloon were used to dilate the tract, with a 30F Amplatz sheath maintaining the open access channel for insertion of a Pentax flexible nephroscope into the intrarenal collecting system. The fiber-optic pH microsensor was placed inside a 5F ureteral catheter (length about 20 inches)—to protect the microsensor and its delicate tip—during its introduction and advancement into the nephroscope's access port. An upper pole calyx was identified for pH measurements during visualization of the collecting system. The microsensor was then advanced outside the protective ureteral sheath and the pig's breathing temporarily suspended for 1–2 min whilst the sensor was inserted into a papillary Bellini duct to measure intraluminal urine pH.

Flexible ureteroscopy was not feasible as an alternative to the PCNL approach as there is no protective sheath available to prevent microsensor damage when placed though the angulated working channel. Also, the ST connector at the meter-end of the fiber-optic cable (see figure 1) prevents back loading into the ureterscope.

SWL-treated Ossabaw MetS pig—Nine-month old female Ossabaw pigs were fed an excess calorie, atherogenic diet to induce obesity and other features of MetS, including the production of overly acidic urine [1, 10, 11]. After 6 months on the hypercaloric diet, the pigs underwent SWL treatment to an upper pole calyx of the left kidney using the unmodified HM3 lithotripter (2000 SWs at 120 SWs/min, 24 kV). Approximately 2 months after SWL, the pigs were prepared for PCNL and pH measurements as described above. The two pigs in the present series of experiments are a subset of the animals assessed for glucose tolerance and insulin resistance before and after SWL in a recently published study [12]. Details of renal function and renal pathology of such SWL-treated MetS pigs has also been published [13].

RESULTS

Calibration of fiber-optic pH microsensor

Fiber-optic microsensors with a tip diameter of 140-μm and tip length of 3-mm were calibrated with six colorless pH buffer solutions (pH 4,5,6,7,8,9) as per the manufacturer's instructions to generate a calibration curve. We also confirmed that placing the fiber-optic microsensor in a small-bore capillary tube (to mimic a collecting duct) during calibration did not influence pH readings. The paired pH buffer value and measured phase angle of each pH buffer solution were entered into the pH Solver-v07 software program to generate a sigmoidal (Boltzmann) curve fit with resulting $phase_{max}$, $phase_{min}$, dpH (slope) and pH_0 (point of inflection) values. Entering these four derived values into the calibration table of the pH meter completes the calibration of the microsensor. We calibrated sixteen fiber-optic

pH microsensors and then measured the acidity of several pH buffers showing excellent linear correlation in the pH 5–8 range between measured and expected pH values [Measured pH = 1.028 (Expected pH) – 0.227, $r^2 = 0.9973$, p = 0.0013; see Figure 2 and Table 1]. These results are in agreement with the manufacturer's claim that the pH microsensor is most accurate in the pH 5.5–8.5 range.

Proof of concept experiment

The sequence of events in obtaining a renal tubule pH measurement is shown in the panels of Figure 3. The nephroscope was advanced into an upper pole calyx revealing a conical shaped papilla (Figure 3A). Openings for two ducts of Bellini are clearly seen at the papillary tip (each duct opening is marked with an ellipse numbered 1 & 2). A bubble (double arrowheads) is adjacent to the second duct of Bellini. The edge of the ureteral catheter (yellow color and marked with a single arrowhead) that protects the microsensor is also seen at the right hand margin of each panel. In Figure 3A the microsensor is within the ureteral catheter. In Figure 3B, the microsensor (enclosed in circle and enlarged in insert) was advanced outside of the protective sheath and then we confirmed that the microsensor was functional by switching the microsensor on and 1) visually observing flashes of light (arrow in Figure 3B and insert) at the microsensor tip, and 2) simultaneously obtaining pH measurements of the fluid within the calyx space. The microsensor was then maneuvered to the opening of the first duct of Bellini (Figure 3C), followed by careful insertion of the microsensor with a 3-mm tip length tip into the duct and the start of tubular fluid pH measurements (Figure 3D). Immediately before and during pH measurements the pig's breathing was suspended for ~1-min to reduce papillary motion. Routine saline irrigation to visualize the collecting system had a pH of ~5.33 (range 5.03–5.73) and was also suspended during tubular pH recordings. Phase angle measurements in the two adjacent Bellini ducts labeled 1 and 2 in Figure 3A gave pH readings of 6.78 and 7.04, respectively. Bulk urine was not collected from the kidney in this experiment, but such farm pigs have a bulk urine pH value of ~7 (unpublished results of urine collected from the ureters of nine pigs using a conventional pH electrode and meter).

Figure 4 shows examples of continuous phase angle and pH values recorded in a Bellini duct in an upper pole papilla. Measurements were recorded each second for as long as the microsensor tip could be held in the tubule to achieve stable phase angle values. A stable reading was considered achieved when the phase angle did not deviate by more than ± 0.1. The results demonstrate that the pH microsensor has a relatively quick response time with phase angle and pH values becoming stable over the recording period. *In vitro* conditioning of the microsensor in pig urine for 10–20 minutes before use appeared to improve the response time to achieve a stable phase angle reading.

SWL-treated Ossabaw MetS pig experiment

Table 2 shows microsensor derived pH values and conventional pH electrode values along the urinary tract of two SWL-treated Ossabaw MetS pigs. Urinary pH values were measured from urine collected from a catheter inserted into the ureter and advanced towards the renal pelvis of the SWL-treated kidney; and tubular urine within papillary Bellini ducts located within the SW-targeted upper pole calyx.

We found in both pigs that there was discordance between pH values measured in Bellini ducts within the SW-treated region of the kidney and bulk urine collected from the ureter of the same renal unit (reflects the integrated pH value of newly formed urine from all tubule ducts in the kidney). Tubule urine from SW-treated regions of the kidney was on the order of 1 pH unit (or greater) higher than urine collected from the entire kidney.

It was difficult to gain access to papillary ducts other than those in the upper pole when employing a lower pole percutaneous access site and flexible nephroscope. Dilation of the infundibulum was necessary to gain access to papillae, which resulted in tearing of tissue and bleeding. This impaired visualization of the tubular ducts especially when the irrigation saline infusion was temporarily suspended to obtain pH recordings.

Ethylene oxide (ETO) sterilization of the fiber-optic pH microsensor

We have independently confirmed that in-house hospital sterilization of eight fiber-optic microsensors with ETO does not significantly influence the calibration curve of the pH microsensor (Figure 5A). Again, we found excellent linear correlation in the pH 5–8 range between measured and expected pH values [Measured pH = 0.9741 (Expected pH) + 0.1531, $r^2 = 0.9991$, $p = 0.0004$; see Figure 5B]. Thus the high resolution of the pH microsensor in the optimal range of pH 5–8 is maintained after ETO sterilization—allowing its potential use in survival animal experiments and human studies.

DISCUSSION

We provide the first report of urine pH measurements within papillary Bellini ducts of a large mammal, performed *in vivo* and in real-time. This was possible due to a fiber-optic phase detection system and very small microsensors. The tubule pH measurements were performed in a large animal model (adult swine) whose Bellini duct opening is sufficiently large for the insertion of the 140-μm diameter microsensor tip. Fiber-optic pH sensing technology has been used *in vivo* in several vertebrate species [14–17] including humans [18–20]. But, to our knowledge this is the first use of such pH sensing technology in renal biology.

The ability to measure pH within renal tubules is highly novel and has the potential to greatly expand our understanding of the etiology of stone formation in human nephrolithiasis. For example, there is discordance between the mineral composition of tubular deposits and renal stones in uric acid, bariatric, ileostomy, and non-bariatric enteric hyperoxaluric stone formers [2]. Such patients will form CaOx or UA renal stones—bulk urine is acidic with high CaOx or UA supersaturation with no evidence of CaP supersaturation—yet their tubular deposits contain CaP (apatite), which only forms in a more alkaline environment. Our demonstration that the high resolution of the fiber-optic pH microsensor is maintained after ETO sterilization will now allow direct testing of whether heterogeneity of tubular pH function exists within the kidneys of such stone formers.

Another example of the potential application of such technology is in issues related to stone treatment. It is well established that SWL can injure the kidney [21, 22] and there have long been discussions that such trauma to the renal parenchyma might affect the subsequent

progression of stone disease [23]. There is epidemiological evidence of an association between the number of prior SWL treatments a patient has undergone and the percentage of CaP within their stones [24]. One hypothesis for this association is that SWL leads to localized renal injury, which in turn impairs tubular acidification mechanisms and creates an alkaline microenvironment favoring CaP stone formation. Optical pH sensing technology will allow the testing of such a hypothesis by measuring intraluminal papillary duct urine pH in SWL-treated regions of the kidney. Indeed, our findings in SWL-treated MetS pigs would support the notion that SWL leads to a chronic alkalinization of tubular urine. The majority of tubules in the MetS pig kidney must have produced acidic urine to account for the highly acidic bulk urine, whereas tubules within SW-treated regions of the same kidney produced less acidic urine that was on the order of 1 pH unit or higher than urine collected from the entire kidney. This is in keeping with our recent report that treating the entire pig kidney with an overdose of 8,000 SWs leads to alkaline bulk urine compared to the opposite nontreated kidney, i.e. an acidification defect in the SW-treated kidney [25]. We have also recently documented remodeling of nephron structures in SWL-treated regions of the kidney, which could potentially impact tubule acidification processes [25, 26]. With the limitations of this current pilot study (see below) it would be premature to draw firm conclusions linking a change in ductal urine pH to injury caused by SWL. Still, our observation of a greater than 1 pH unit difference between intraluminal urine in the SWL-treated regions of the kidney versus bulk urine from the same renal unit is intriguing and merits further investigation.

The procedure to measure pH in tubular ducts is demanding requiring great dexterity to enter and maintain the microsensor in a tubule until a stable phase angle reading is obtained. The success rate in obtaining tubule urine pH measurements was low (~50%) with failure rates largely due to the delicate sensor cap on the fiber-optic tip being dislodged during attempted entry into the tubule. Undoubtedly, there is a learning curve in making such tubule measurements and our expectation is that success rates will rise with experience.

Despite the many limitations (e.g. renal anatomy of the Ossabaw pig made it extremely challenging to perform tubule measurements using the percutaneous approach; few intraluminal pH measurements could be made because of the low success rates of the microsensor approach) and preliminary nature of our study, the findings suggest that optical sensing technology is a viable option worth pursuing to measure intraluminal pH within papillary ducts of large mammals. The results of our study should be viewed as exploratory in nature.

In conclusion, we provide details on adapting an optical pH sensing technology to measure proton concentration in tubule urine in real time, *in vivo*. This technology has the potential to greatly expand our understanding of kidney stone disease and treatment as the sensor can be tailored to measure proton concentration and/or other analytes relevant to stone formation.

Acknowledgments

Drs. Ehud Gnessin and Jessica Mandeville aided in the percutaneous access surgery with JEL inserting fiber-optic microsensors into Bellini ducts. RKH operated and evaluated the performance of the fiber-optic phase detection

system. The authors are grateful to Dr. James A. McAteer for insightful comments on the manuscript, and to Philip M. Blomgren for preparing illustrations.

Funding: Supported by Public Health Service grants P01-DK56788 and P01-DK43881.

References

1. Wagner CA, Mohebbi N. Urinary pH and stone formation. J Nephrol. 2010; 23(S16):S165–S169. [PubMed: 21170875]
2. Coe FL, Evan AP, Lingeman JE, et al. Plaque and deposits in nine human stone diseases. Urol Res. 2010; 38:239–247. [PubMed: 20625890]
3. Sonnenberg H, Chong C. Comparison of micropunture of microcatheterization in papillary collecting duct. Am J Physiol. 1980; 239:F95–F105. [PubMed: 7395998]
4. Graber ML, Bengele HH, Schwartz JH, et al. pH and PCO_2 profiles of the rat inner medullary collecting duct. Am J Physiol. 1981; 241:F659–F668. (Renal Fluid Electrolyte Physiol 10). [PubMed: 6798882]
5. DuBose TD Jr, Lucci MS, Hogg RJ, et al. Comparison of acidification parameters in superficial and deep nephrons of the rat. Am J Physiol. 1983; 244:F497–F503. (Renal Fluid Electrolyte Physiol 13). [PubMed: 6405628]
6. Wolfbeis OS. Fiber-optic chemical sensors and biosensors. Anal Chem. 2008; 80:4269–4283. [PubMed: 18462008]
7. Kocincova AS, Borisov SM, Krause C, et al. Fiber-optic microsensors for simultaneous sensing of oxygen and pH, and of oxygen and temperature. Anal Chem. 2007; 79:8486–8493. [PubMed: 17948966]
8. German Patent Application DE. 198.29.657. 1997 Aug 1.
9. Handa RK, Matlaga BR, Connors BA, et al. Acute effects of percutaneous tract dilation on renal function and structure. J Endourology. 2006; 20:1030–1040.
10. Abate N, Chandalia M, Cabo-Chan AV Jr, et al. The metabolic syndrome and uric acid nephrolithiasis: novel features of renal manifestation of insulin resistance. Kidney International. 2004; 65:386–392. [PubMed: 14717908]
11. Maalouf NM, Cameron MA, Moe OW, et al. Low urine pH: A novel feature of the metabolic syndrome. Clin J Am Soc Nephrol. 2007; 2:883–888. [PubMed: 17702734]
12. Handa RK, Evan AP, Connors BA, et al. Shock wave lithotripsy targeting of the kidney and pancreas does not increase the severity of metabolic syndrome in a porcine model. J Urology. 2014; 192:1257–1265.
13. Handa RK, Johnson CD, Connors BA, et al. Shock wave lithotripsy does not impair renal function in a swine model of metabolic syndrome. J Endourology. 2014
14. McKinley BA, Morris WP, Parmley CL, et al. Brain parenchyma PO_2, PCO_2, and pH during and after hypoxic, ischemic brain insult in dogs. Critical Care Medicine. 1996; 24:1858–1868. [PubMed: 8917037]
15. Devlieger R, Gratacós E, Wu J, et al. Continuous monitoring of fetal pH, pO2 and pCO2 using a fiberoptic multiparameter sensor in animal models reproducing in utero conditions. Fetal Diagn Ther. 2000; 15:127–131. [PubMed: 10781994]
16. Soller BR, Heard SO, Cingo NA, et al. Application of fiberoptic sensors for the study of hepatic dysoxia in swine hemorrhagic shock. Crit Care Med. 2001; 29:1438–1444. [PubMed: 11445705]
17. Ziemann AE, Schnizler MK, Albert GW, et al. Seizure termination by acidosis depends on ASIC1a. Nat Neurosci. 2008; 11:816–822. [PubMed: 18536711]
18. Doppenberg EMR, Zauner A, Bullock R, et al. Correlations between brain tissue oxygen tension, carbon dioxide tension, pH, and cerebral blood flow-a better way of monitoring the severely injured brain. Surg Neurol. 1998; 49:650–654. [PubMed: 9637626]
19. Jauniaux E, Watson A, Ozturk O, et al. In-vivo measurement of intrauterine gases and acid-base values early in human pregnancy. Human Reproduction. 1999; 14:2901–2904. [PubMed: 10548645]

20. Soller BR, Hagan RD, Shear M, et al. Comparison of intramuscular and venous blood pH, PCO_2 and PO_2 during rhythmic handgrip exercise. Physiol Meas. 2007; 28:639–649. [PubMed: 17664618]

21. Evan, AP.; Willis, LR. Extracorporeal shock wave lithotripsy: complications. In: Smith, AD., et al., editors. Smith's textbook on endourology. Hamilton: BC Decker Inc.; 2007. p. 353-365.

22. McAteer JA, Evan AP. The acute and long-term adverse effects of shock wave lithotripsy. Seminars in Nephrology. 2008; 28:200–213. [PubMed: 18359401]

23. Krambeck AE, Handa SE, Evan AP, et al. Brushite stone disease as a consequence of lithotripsy. Urol Res. 2010; 38:293–299. [PubMed: 20623223]

24. Parks JH, Worcester EM, Coe FL, et al. Clinical implications of abundant calcium phosphate in routinely analyzed kidney stones. Kidney International. 2004; 66:777–785. [PubMed: 15253733]

25. Evan AP, Coe FL, Connors BA, et al. Mechanism by which shock wave lithotripsy can promote formation of human calcium phosphate stones. Am J Physiol Renal Physiol. 2015; 308:F938–F949. [PubMed: 25656372]

26. Handa RK, Liu Z, Connors BA, et al. Effect of renal shock wave lithotripsy on the development of metabolic syndrome in a juvenile swine model: A pilot study. J Urol. 2015; 193:1409–1416. [PubMed: 25245490]

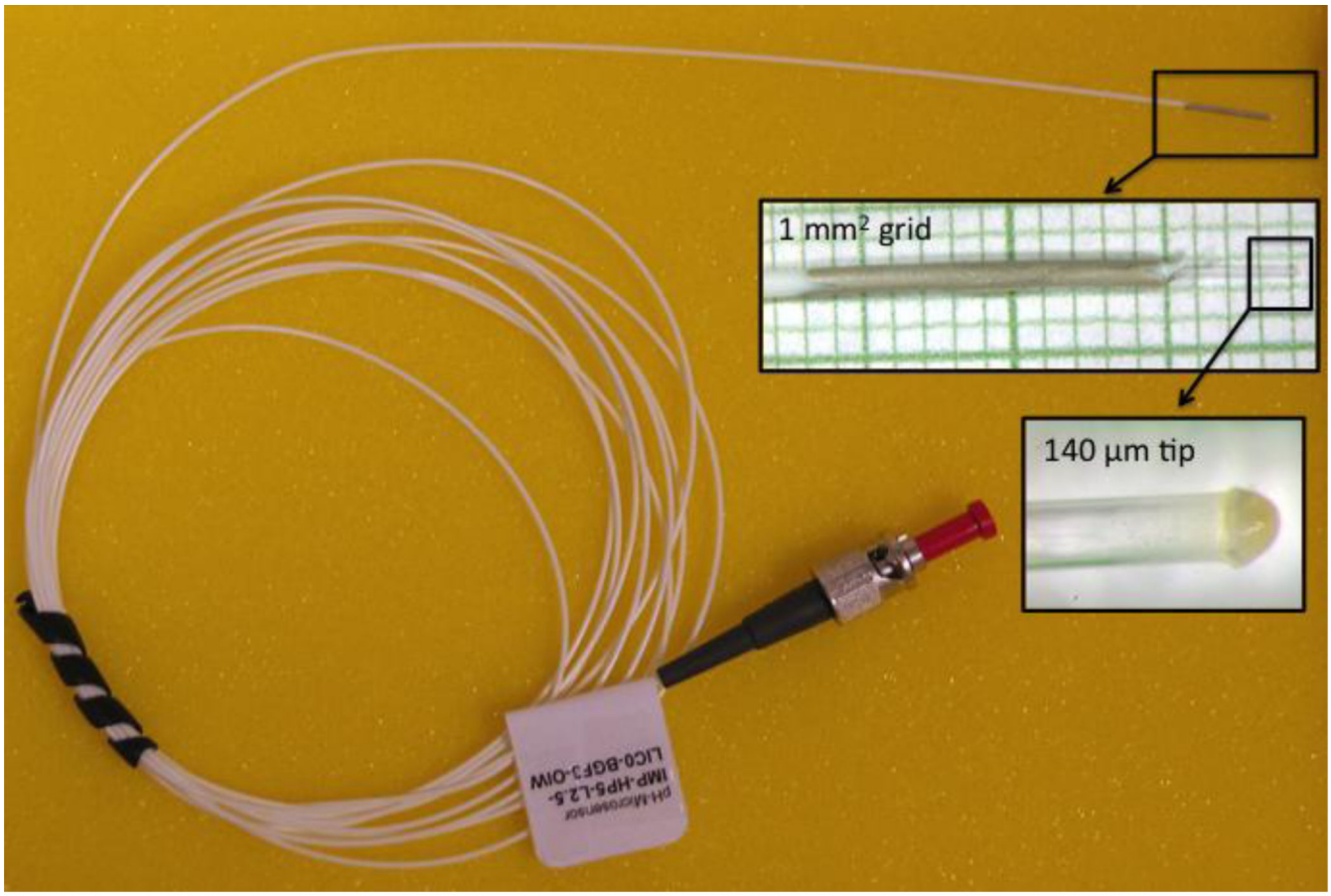

Figure 1.
Fiber-optic microsensor.

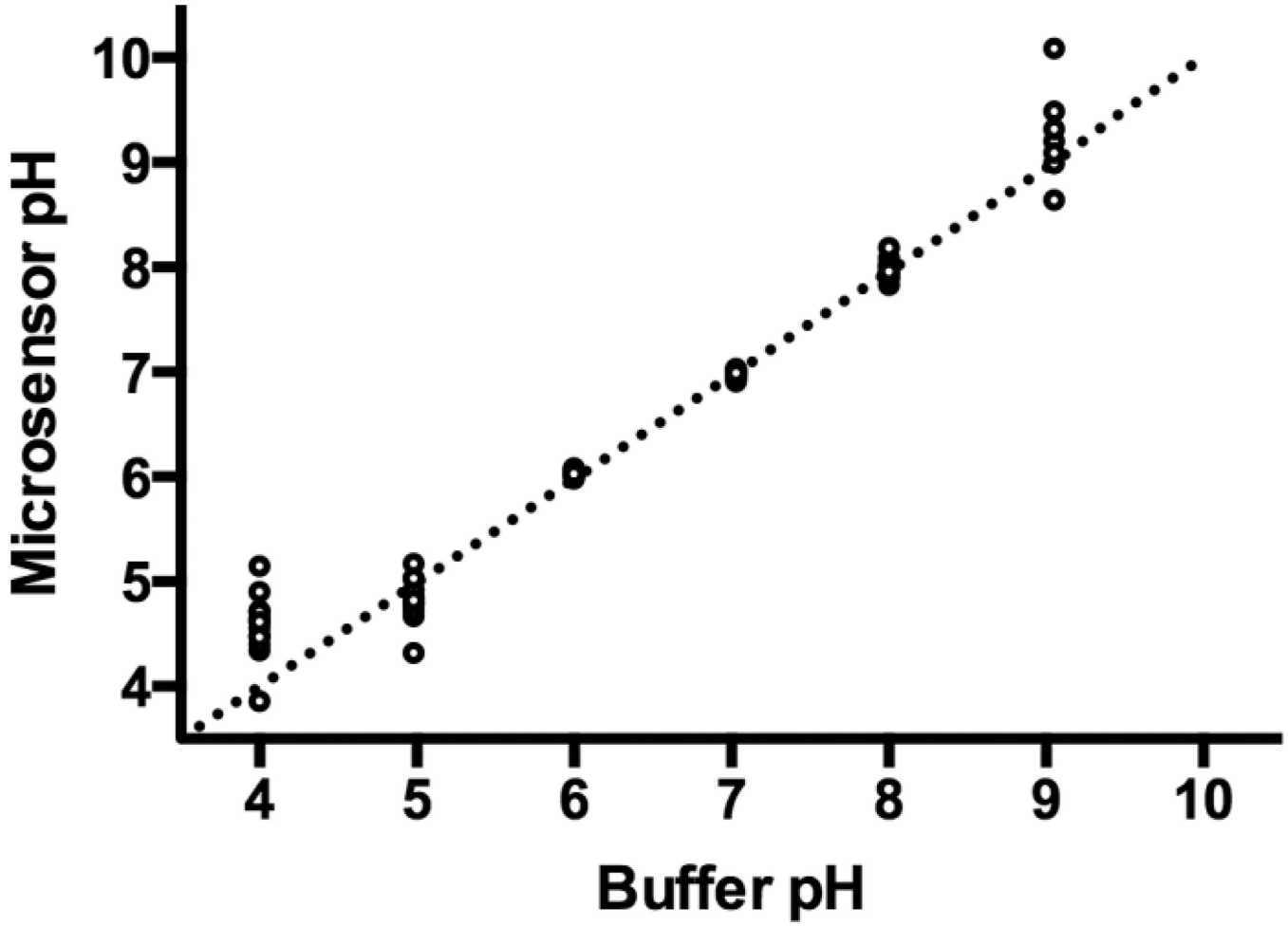

Figure 2.

Measurements of buffer pH solutions using the fiber-optic phase detection system. Each open circle at a particular buffer pH represents a single measurement from one microsensor (see Table 1). Identity line is shown.

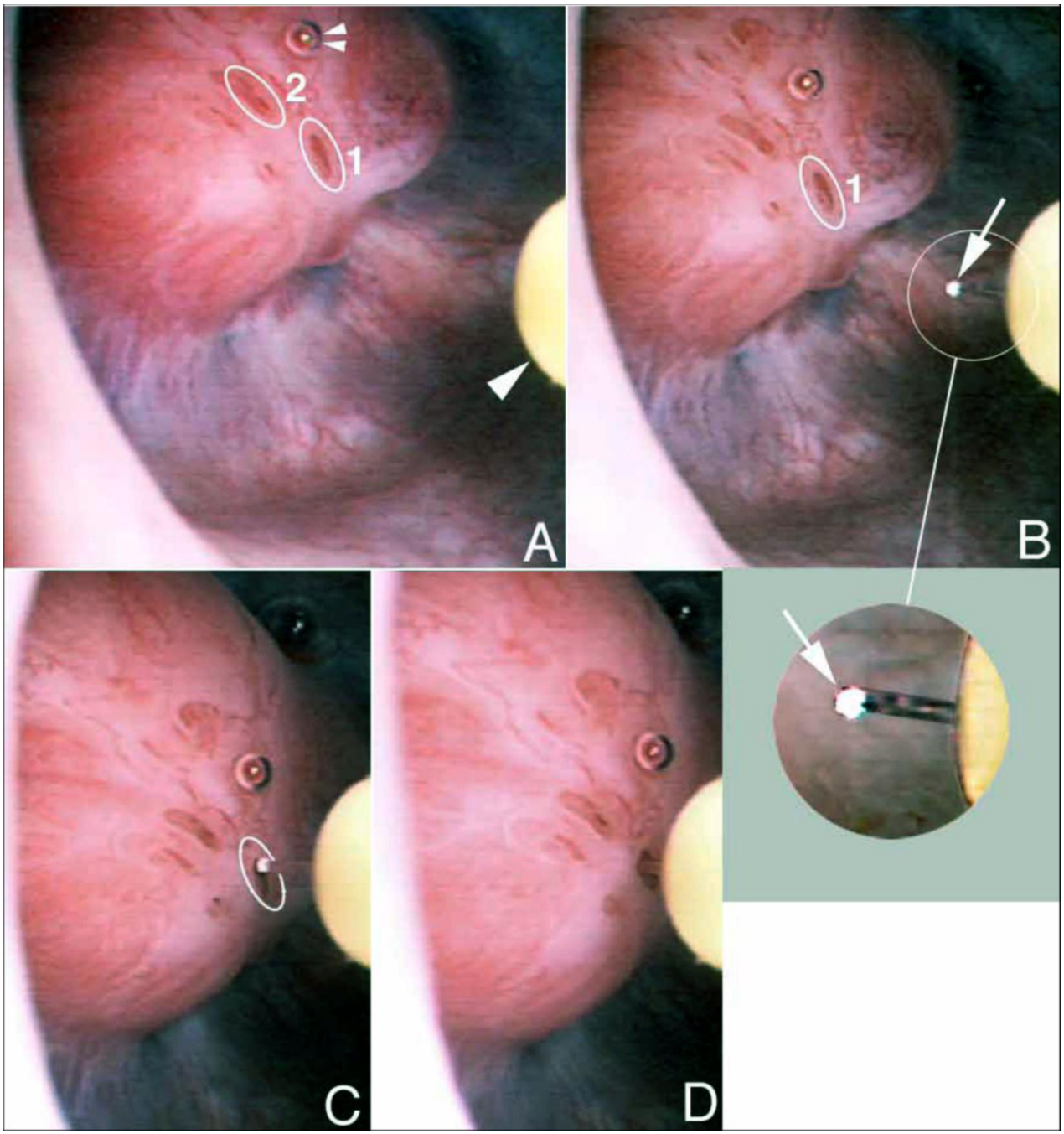

Figure 3.
Sequence of events involved in measuring tubule urine pH (see text in Results section).

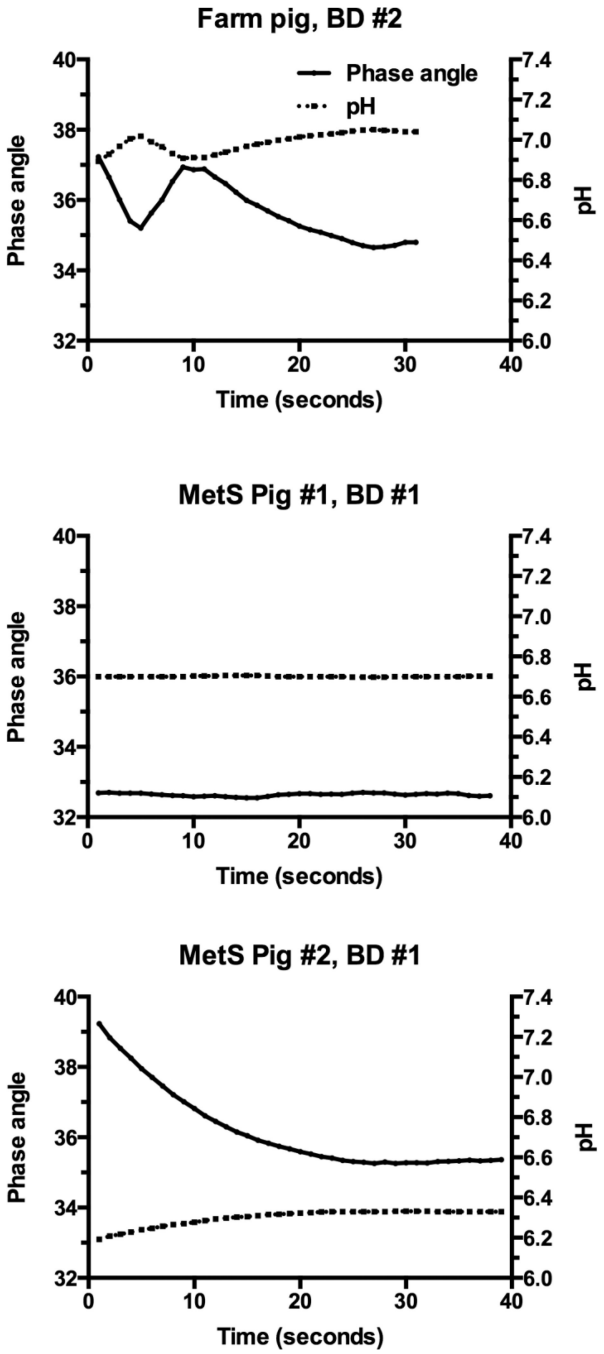

Figure 4.

Shown are examples of phase angle and derived pH values from microsensors in Bellini ducts. Note that fluctuations in phase angle values prior to a stable reading resulted in only small changes in pH values.

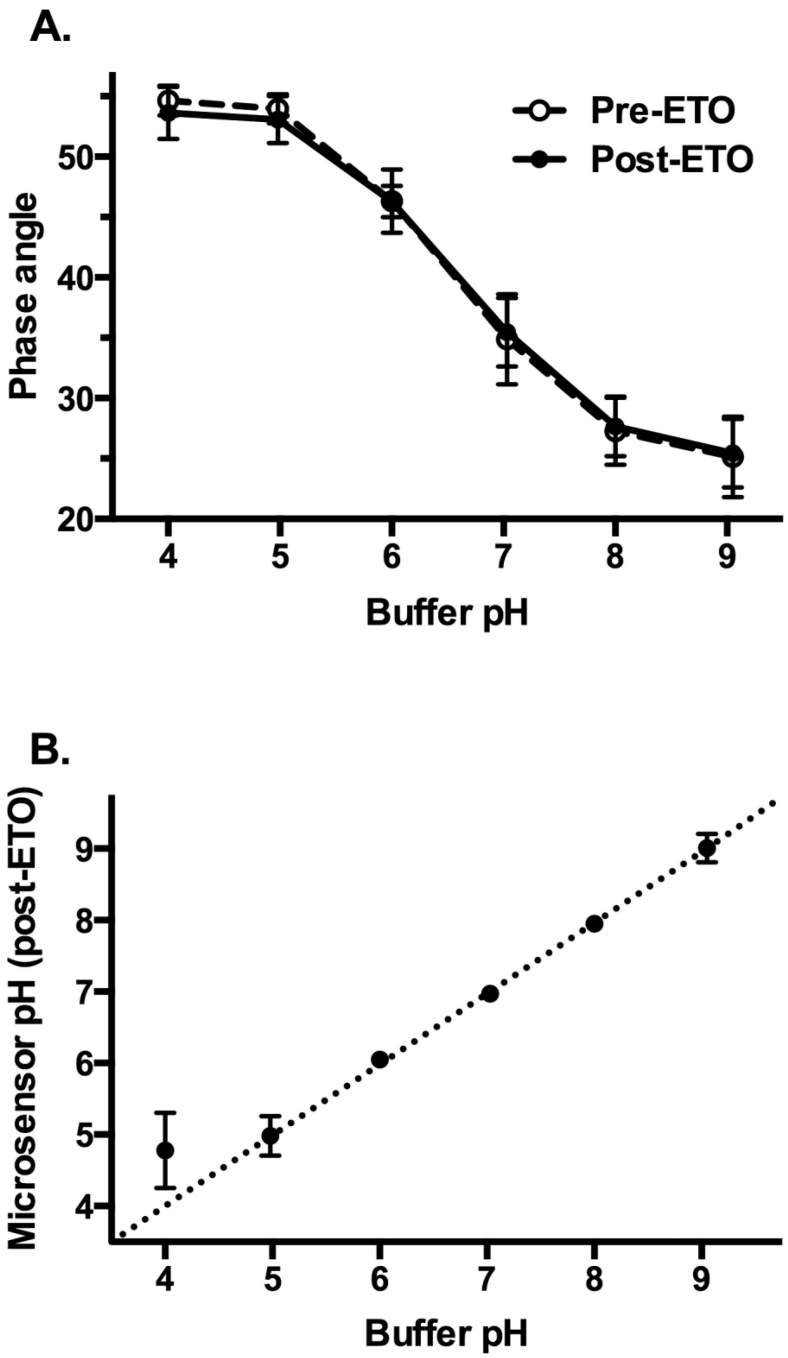

Figure 5.

Shown are microsensor phase angle values of buffer pH solutions before and after ETO sterilization (panel A). Microsensor derived pH values of buffer pH solutions after ETO sterilization (panel B). Mean ± SD values and identity line are shown.

TABLE 1

Buffer solution pH	4.0 ± 0.1	4.98 ± 0.1	6.0 ± 0.1	7.03 ± 0.1	8.0 ± 0.1	9.05 ± 0.1
Microsensor pH	4.58 ± 0.27	4.83 ± 0.19	6.04 ± 0.03	6.99 ± 0.03	7.97 ± 0.09	9.26 ± 0.45
N =	16	16	16	16	16	7

Mean ± SD values are shown at 20°C. N = number of observations.

Urolithiasis. Author manuscript; available in PMC 2017 June 01.

TABLE 2

	Location	Microsensor ID #	Microsensor pH	Electrode pH
MetS pig #1:				
SWL-treated kidney	Ureter	11	5.80	6.00
SWL-treated kidney	UP, P #1, BD #1	11	6.70	N/A
MetS pig #2:				
SWL-treated kidney	Ureter	10	5.19	5.33
SWL-treated kidney	UP, P #1, BD #1	10	6.33	N/A
SWL-treated kidney	UP, P #1, BD #2	10	6.40	N/A

UP = upper pole; P = papilla; BD = Bellini duct; N/A = not applicable.